RSC Advances

ROYAL SOCIETY OF CHEMISTRY

www.rsc.org/advances

Journal Name

ARTICLE

Novel composite membranes of triazole modified graphene oxide and polybenzimidazole for high temperature polymer electrolyte membrane fuel cell applications

Received 00th January 20xx,
Accepted 00th January 20xx

DOI: 10.1039/x0xx00000x

www.rsc.org/

Jingshuai Yang, Chao Liu, Liping Gao, Jin Wang, Yixin Xu, Ronghuan He*

Simultaneously improving the proton conductivity and mechanical property of the polymer electrolyte, especially to phosphoric acid doped membranes, is a challenge for preparation of membrane materials in application in the proton exchange membrane fuel cells. We prepared a novel composite membrane by introducing triazole functionalized graphene oxide into the polybenzimidazole for using as the high temperature proton exchange membrane. Increases in both proton conductivity and tensile strength were achieved by the composite membrane compared with the pure PBI membrane after doped with phosphoric acid. The triazole modified graphene oxide could disperse well in the polar organic solvent, which resulted in easy fabrication of the homogeneous membranes. The proposed material is of a demonstration for designing and preparing inorganic composite polymer electrolytes with superior properties.

1. Introduction

High temperature proton exchange membranes (HT-PEMs) have attracted much attention due to the technical advantages for practical utilization of proton exchange membrane fuel cells (PEMFCs), such as high reaction kinetics at both anode and cathode, less catalyst poisoning at the anode, and easy heat and water managements of the stacks.[1,2] Among HT-PEMs, phosphoric acid (PA) doped polybenzimidazole (PBI) is the most attractive one since the doped PA allows the membrane to achieve high proton conductivity at temperatures above 100°C without humidification,[1, 3, 4] although various sulfonated PBIs[5,6] have also been proposed as proton conducting membranes. Normally, the conductivity of PBI/PA membranes highly depends on the acid doping level (ADL, the mole number of PA per mole PBI repeat unit), and can be significantly improved by increasing the PA content of the membranes.[7] However, a very high PA acid content brings a significant deterioration in the mechanical strength of the electrolyte due to the plastic effect of the doping PA[8,9], especially at elevated temperatures.

In order to improve the mechanical properties of PBI based HT-PEMs, the composite PBI membranes have been developed by incorporating of inorganic fillers such as nano silica,[10-13] titanium,[14] clay compounds[15] and nano carbon materials[16-19]. Generally, the dispersion of the inorganic fillers and the compatibility of the membrane components significantly affect the properties of the composite membranes in terms of e.g. dimensional stability, mechanical properties and gas permeability. In addition, most of the reported PBI composite membranes with inorganic fillers show reduced proton conductivities as the presence of inorganic materials dilutes the concentration of proton-conducting groups.[11] To improve the compatibility of inorganic fillers and polymers for homogeneous membranes, approaches including modification of inorganic fillers with various organic groups and use of nano scale inorganic materials have been reported.

Graphene oxide (GO), which is exfoliated from graphite oxide nanoplatelets, has attracted increasing attention these years, mainly due to its advantages of excellent mechanical properties, large specific surface area, and low cost.[20] It was recently reported that GO sheets exhibited proton conductivities as high as 10^{-2} S cm^{-1} because of the presence of the hydrophilic oxygen-containing groups attached to the graphene sheets.[21] Those groups include carboxylic acid and epoxy oxygen, which could facilitate hopping of protons through hydrogen-bonding networks in association with water molecules. This investigation motivated us to construct GO assistant proton conducting networks in PBI/PA membranes and meanwhile to improve the tensile strength of PBI membranes. However, the poor degree of dispersion of GO in organic solvents results in a difficulty for forming a homogeneous composite membrane. As previously reported, modifications of GO via grafting various organic groups on the surface of its structure have been proved as the effective method to improve the compatibility between GO and the polymer matrix. The organic compounds, such as 3-mercaptopropyl trimethoxysilane,[22] 1-aminopropyl-3-methyl-imidazole[23], *p*-aminobenzene sulfonic acid[24], ionic liquid

Department of Chemistry, College of Sciences, Northeastern University, Shenyang 110819, China. Email: herh@mail.neu.edu.cn. Fax: +86-24-83676698; Tel.: +86-24-83683429.
Electronic Supplementary Information (ESI) available: [details of any supplementary information available should be included here]. See DOI: 10.1039/x0xx00000x

polymer [25] and polydopamine [26] et al., were proposed to organically modify GO through a nucleophilic reaction between the epoxy group in GO and the amine group in organics.

In the present work, triazole modified graphene oxide (MGO) was synthesized and used as the filler to fabricate PBI composite membranes. We presumed that the presence of the triazole groups could help the MGO to uniformly disperse in the composite membrane for an enhanced tensile strength. Meanwhile, the grafted triazole groups were supposed to benefit the proton conduction by forming hydrogen-bonding networks with PA. Thus novel composite PBI membranes with the MGO were expected to achieve excellently comprehensive properties as the membrane electrolyte at elevated temperatures.

2. Experimental

2.1 Synthesis of GO and MGO

GO was prepared by oxidation of the graphite powder (purchased from Sigma-Aldrich) with a modified Hummers' method and the product was purified by centrifugation.[27] MGO was synthesized by introducing 3-amino-1,2,4-triazole (Am-Tri, Sigma-Aldrich) onto graphene oxide via an epoxide ring-opening reaction or a neutralization reaction with carboxylic acids according to the similar rout previously reported,[28,29] as shown in Fig. 1. Typically, in 500 mL round bottom flask, 100 mg of GO was homogeneously dispersed in 200 mL of deionized water. Then 200 mg 3-amino-1,2,4-triazole and 200 mg KOH were added, followed by ultrasonication for 1 h. The mixture was transferred to an oil bath for refluxing at 80 ^{o}C for 24 h under stirring to obtain a homogeneous black solution as shown in Fig. 1. After centrifugation at 5000 r min^{-1} for 30 min, the resulted solution was transferred to a dialysis bag and neutralized by dialysis with neutral water for 7 d. The black powder of MGO was obtained after drying under vacuum at room temperature for 7 d.

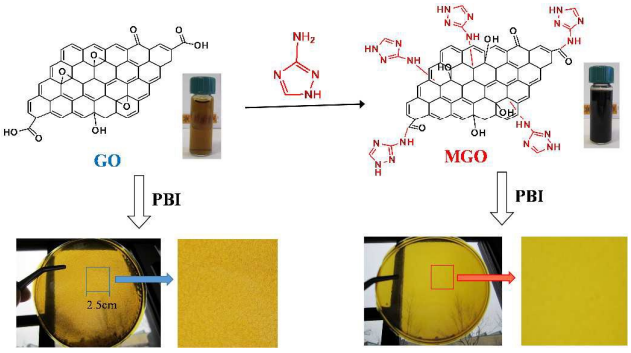

Fig. 1 Schematic of the preparation process of MGO and PBI based composite membranes; and photos of GO and MGO aqueous solutions as well as PBI based composite membranes

2.2 Preparation of composite membranes and acid doping

The PBI polymer having a molecular weight of around 37 kg mol^{-1} was synthesized according to a previously reported procedure.[30] The prepared PBI polymer and MGO powder were dissolved in *N,N*-dimethylacetamide (DMAc) with a concentration of 2 wt%, respectively. The two solutions were mixed with a MGO mass percent of 1.2% and then ultrasonicated for 2 h. The mixture of PBI and MGO was poured onto a Petri dish, followed by drying at 80 ^{o}C for 3 h and at 120 ^{o}C for 21 h. The resulting membranes were then peeled off and soaked in deionized water at 80 ^{o}C for 1 h and further dried at 180^{o}C for 2 h. For comparison, pristine PBI and PBI with GO membranes were prepared similarly. For acid doping, membranes were imbibed with phosphoric acid in 80 or 85 wt% PA solutions at room temperature for one week. The ADL was calculated from the mass gains of the membranes after the acid doping procedure and defined as the mole number of PA per mole of PBI repeat unit, taking into account of no absorption of PA in organic fillers.

2.3 Characterizations and fuel cell measurement

The Fourier transform infrared spectra (FT-IR) of GO and MGO were recorded with a Bruker VERTEX70 spectrometer to identify characteristic groups in their structures. The XPS was made using a Thermo ESCALAB 250Xi system with Al Kα radiation. The shift of the binding energy due to relative surface charging was corrected using the C 1s level at 284.8 eV as an internal standard. The thermal properties of inorganic materials (GO and MGO) and membranes (PBI and PBI/MGO) were evaluated by thermogravimetric analysis (TGA, HT/808, METTLER-TOLEDO), in air and N_2 atmosphere with a heating rate of 10 ^{o}C min^{-1}, respectively. The morphology of GO and MGO was observed by transmission electron microscopy (TEM, JEM 1200EX, Japan). The surface and cross section of membranes were observed on a scanning electron microscopy (SEM, Ultra Plus). A method of four-probe (made of platinum) was used to determine the conductivity of the membranes, using alternative current with a frequency of *ca* 2 kHz. The mechanical strength of the membranes was measured with a tensile strength instrument (CMT6502, SANS Company, China). The measurements on conductivity and mechanical strength were performed under non humidification.

The membrane-electrode assemblies (MEAs) with an active electrode area of 6.25 cm^2 were fabricated at a temperature of 150 ^{o}C and a pressure of 2 MPa for duration of 5 min. The electrode was prepared according to the previous work,**9** and the platinum loading was about 0.6 mg cm^{-2} for each electrode. Hydrogen and oxygen at flow rates of 120 and 60 mL min^{-1}, respectively, were supplied to the fuel cell without any pre-humidification. Polarization curves were obtained using a current step potentiometry.

3. Results and discussion

3.1. Synthesis of GO and MGO

GO platelets exhibit chemically reactive oxygenic functionalities, such as carboxylic acid groups at their edges, and epoxy and hydroxyl groups on the basal planes, according to the widely accepted Lerf–Klinowski model.[31] Due to the presence of epoxy groups, nucleophilic substitution of epoxides with amino-groups containing molecules towards functionalized GO could be achieved.

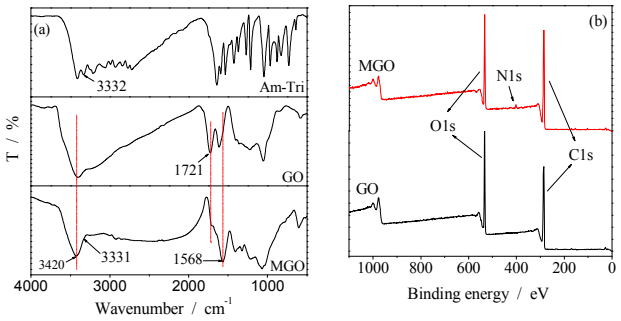

Fig. 2 FTIR (a) and XPS (b) spectra of GO and MGO

The structural information of GO and MGO was determined via FTIR and XPS spectra as shown in Fig. 2. The characteristic peaks of the O–H and C=O stretching vibrations were observed at 3420 and 1721 cm^{-1} in the spectrum of GO, respectively.[25,32] Compared to the FTIR spectrum of GO, that of MGO showed a decreased absorption of C=O stretch at 1721 cm^{-1} as shown in Fig. 2(a), confirming deoxygenation of the GO after the chemical reduction. A new band corresponding to the C=N was observed at 1568 cm^{-1} in the spectrum of MGO, indicating successful modification of the GO. For comparison, the FTIR spectrum of the Am-Tri is also shown in Fig. 2. The adsorption of N–H at around 3330 cm^{-1} appeared in the spectra of both MGO and Am-Tri, which confirmed the reaction between GO and Am-Tri as well. Fig. 2b provides the XPS spectra of GO and MGO from 0 to 1100 eV. Besides the notable peaks at binding energy of 285 eV for C 1s and 531 eV for O 1s, a new peak at around 401 eV originating from triazolegroups was observed in the spectrum of MGO.[29] In addition, the TGA data also proved that triazole was introduced onto the GO structure as seen in Fig. S1 (ESI). The weight loss of the MGO at around 200 ^{o}C was obviously lower than that of the GO, indicating a decreased amount of oxygenated functional groups.[26,29]

The nanosheet structure and morphology of GO and MGO were further investigated by TEM images as displayed in Fig. 3. TEM analysis (Fig. 3(a) and (b)) showed that the pristine graphene oxide nanosheets appeared relatively flat with some wrinkles, which is consistent with the typical morphology reported in the literature.[22,28] After reacted with triazole, MGO still maintained the shape of thin sheets as well.

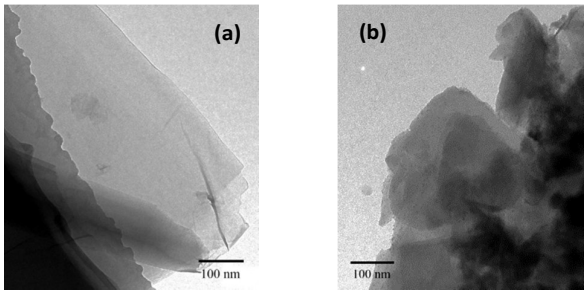

Fig. 3 TEM images of GO (a) and MGO (b)

3.2. Preparation of PBI based composite membranes

Generally GO has a poor dispersion in common organic solvents. Nevertheless, MGO has a good dispersion in DMAc and exhibits an excellent compatibility with PBI. As seen from the photographs in Fig. 1, MGO in the PBI/MGO membrane was well-distributed and the resulted PBI/MGO composite membrane was transparent and uniform. However, the PBI/GO membrane showed a rough and phase-separated appearance. Fig. 4 shows the distribution of the filler in the PBI membrane as determined by SEM. No entangled or aggregated MGO particles appeared in the SEM images, indicating the almost complete and homogeneous dispersion of MGO in the PBI matrix. The well dispersed MGO in the polymer was obviously due to the chemical affinity of the triazole-based groups with the polymer network. Meanwhile, the PBI/MGO membrane is essentially non-porous and dense, which should minimize hydrogen or oxygen gas crossover during fuel cell operation and benefit the fuel cell performance. For the PBI/GO membrane, some obvious particles appeared on the surface of the PBI/GO membrane as seen from Fig. 4 (e) and (f), which should result from the aggregation of GO. The weak interaction and inferior compatibility between PBI and GO might bring on the micro-phase separation and the aggregation of GO.[26]

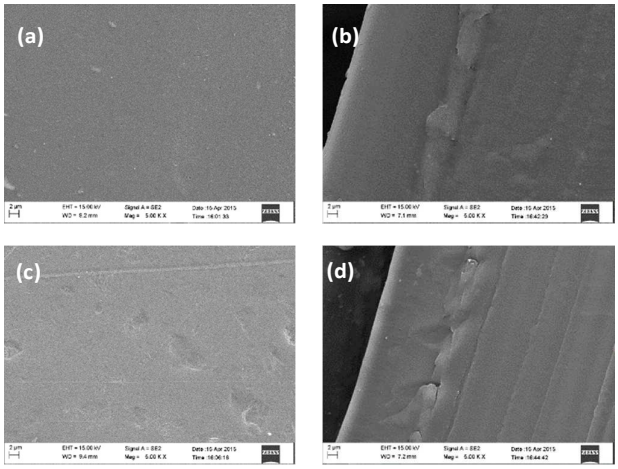

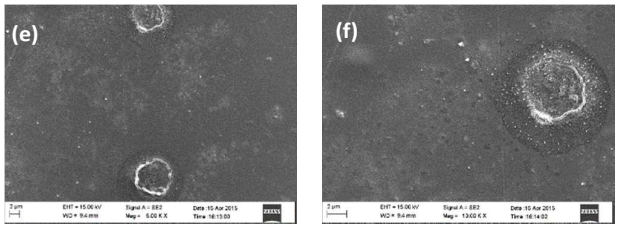

Fig. 4 SEM images of the pristine PBI (a-surface, b-cross-section, ×5000), PBI/MGO (c-surface, d-cross-section, ×5000) and the PBI/GO (e-surface: ×5000, f-surface: ×10000) membranes

In addition, the thermal stability of membranes was identified by TGA as shown in Fig. S1. The almost the same TGA curves of the two membranes suggest that the PBI/MGO is as thermally stable as the PBI for suitable application at elevated temperatures. The mass loss below 200 °C resulted from the absorbed water in the membrane. The slightly higher mass loss of PBI than that of PBI/MGO below 200 °C is in good agreement with the results of water uptake of the membranes at 20°C, i.e., 9.9% for PBI and 6.7% for the PBI/MGO membrane, respectively.

3.3. Conductivity and mechanical properties

The proton conductivities under anhydrous conditions and mechanical stress-strain curves at room temperature of acid doped pure and composite PBI membranes are shown in Fig. 5, respectively. As seen from the Fig. 5 (a), the incorporation of MGO sheets into the polymer membranes resulted in a considerable increase in the proton conductivity of the membranes compared to the PBI membrane under the similar ADL of around 12. The triazole groups in MGO could form the hydrogen-bonding with the doping acids, which might provide effective pathways for proton transfer. Ye et. al. observed similar results for graphene-modified protic ionic liquid-based composite membranes.[25] They attribute this improvement on ion conductivity to facilitation of ion transport on the external surfaces and formation of 3D ion transport channels throughout the membrane. In order to know the contribution of the introduced Am-Tri on the proton conduction of the composite membrane, the same mass percent (1.5%) of Am-Tri as that of MGO was used to fabricate PBI/Am-Tri/12.0PA membranes. As seen in Fig. 5(a), the conductivities of the PBI/Am-Tri/12.0PA membrane were obviously lower than those of the PBI/MGO/12.2PA membrane, and were comparable to those of PBI/12.3PA below 160 °C. A slight difference in the conductivity was observed between PBI/12.3PA and PBI/Am-Tri/12.0PA membranes at temperatures from 160 to 180 °C, which apparently resulted from the small difference in the acid doping level. The results indicate that the presence of 1.5% Am-Tri has no significant influence on the proton conductivity of the composite membrane. However, Am-Tri groups could not only benefit the formation of the homogeneous composite membrane as discussed above, but also enhance the conductivity of the membrane when it was introduced onto GO to form MGO. Nevertheless, further investigations are needed to better understand the mechanism. The enhancement in the mechanical properties of the PBI/MGO composite membranes was also observed as shown in Fig. 5(b). The tensile strength, elongation and Young's modulus of PBI/MGO/12.2PA were 12.6 MPa, 150.1% and 35.7MPa, respectively. The excellent reinforcement of mechanical properties for PBI/MGO composite membranes could be attributed to the good dispersion of MGO sheets in the composite membranes and the strong interactions between the MGO and the polymer matrix.[24-26]

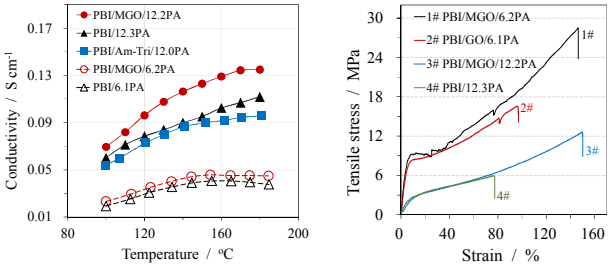

Fig. 5 Conductivities as a function of temperature (a) and tensile stress-strain curves at RT (b) of acid doped PBI and PBI/MGO membranes with different ADLs

The conductivities and mechanical properties of PBI/MGO/12.2PA as well as those from literatures are summarized in Table 1 for comparison. As seen in Table 1, the proton conductivities of PA doped PBI/MGO are significantly higher than those of other modified-GO-based composite HT-PEMs. The superior properties of conductivity and tensile strength over those of the pristine PBI membrane indicate that the PBI/MGO composite membrane is a suitable candidate for use in fuel cells.

Table 1 Summary of conductivity and mechanical properties of HT-PEMs composited with functionalized GO

Membrane	Conductivity /S cm^{-1}		Mechanical property at RT	
	160 °C	180 °C	Strength /MPa	Elongation / %
PBI/MGO/ 12.2PA	0.129	0.135	12.6	150.1
PBI/ILGO[a]/ 3.5PA[23]	-	0.034	-	-
BuPBI/iGO[b] (10%)/PA[33]	0.025	-	-	-
QPEEK[c]/ 3%FGO/PA[24]	0.048	0.053	30.0	120.0
PBI/SGO[d]/ PA[18]	-	0.052	-	-

a: ionic-liquid-graphite-oxide; b: isocyanate modified graphene oxide; c: quaternized poly(ether ether ketone); d: sulfonated graphite oxide.

3.4. Fuel cell performance

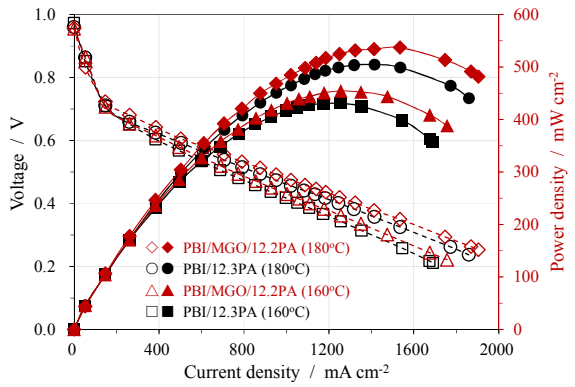

Fig. 6 Polarization and power density curves of the fuel cells operated at 160 and 180 °C with anhydrous H_2/O_2 under atmospheric pressure. Pt loading: 0.6 mg cm^{-2}.

Fuel cell tests based on PA doped PBI/MGO/12.2PA and PBI/12.3PA membranes were performed with un-humidified H_2/O_2 at atmospheric pressure as shown in Fig. 6. The open circuit voltages (OCVs) of all membranes were at the range of 0.96-0.97 V. The high OCVs indicated that the membranes were densely compacted and thus exhibited the low gas crossover, which was already confirmed by the SEM images. The fuel cell performance increased as the increase of the temperature for all the membranes due to increased conductivity and electrode kinetics. The performance of the cells based on the PBI/MGO composite membrane was better than that of the PBI membrane at the similar ADL of around 12. For instance, the peak power densities at 180 °C were 537 mW cm^{-2} for PBI/MGO/12.2PA and 506 mW cm^{-2} for PBI/12.3PA, respectively. The improved performance was mainly attributed to the superior proton conductivity of the hybrid membrane. Meanwhile, the open circuit voltage (OCV), the cell voltage at a current loading of 600 mA cm^{-2} and the polarization curve of the MEA based on the PBI/MGO/12.2PA membrane were recorded at 160 °C and the results are shown in Fig. S2. The MEA displayed almost the same fuel cell performance at different measurement point, and no obvious degradation was observed within the test period. However, it should be noted that much longer life time measurement should be carried out to evaluate the performance of a membrane electrolyte for practical applications in the fuel cell setup as reported in literatures.[30, 34] In addition, the gas diffusion electrode was made using PBI as the catalyst binder, which means it was more suitable for the PBI membrane rather than the organic-filler composited PBI membrane. Thus, it is reasonable to expect better fuel cell performance if the electrode structure and MEA fabrication were optimized. In addition, studies on the mechanisms of enhancement of the properties of the PBI/MGO/PA membrane by MGO and its optimized concentration should be made in the future work.

Conclusions

Novel PBI composite membranes with well-dispersed triazole-modified graphene oxide (GO) were prepared. The triazole groups were successfully grafted onto the surface of GO according to the FTIR, XPS, TGA and TEM results. The modified graphene oxide (MGO) by triazole exhibited excellent distribution in DMAc and possessed improved compatibility with the PBI polymer. The SEM images obviously illustrated that PBI/MGO membranes with a MGO percent of 1.2 wt% were uniform and homogeneous, while PBI/GO membranes were heterogeneous with obvious phase-separation. High proton conductivity of 0.135 S cm^{-1} at 180 °C was achieved by the phosphoric acid (PA) doped PBI/MGO membrane. The triazole groups in MGO interacted with the doped acid PA to form hydrogen bonds, which thus facilitated the proton conduction in the composite membrane. The tensile strength of the PA doped composite membrane was 12.6 MPa at room temperature, which was much higher than that of the PBI membrane with a similar ADL of around 12. At 180 °C, the fuel cell based on the PBI/MGO/12.2PA membrane achieved a peak power density of 537 mW cm^{-2}. The proposed material is of a demonstration for designing and preparing composite polymer electrolytes with superior properties by introducing inorganic fillers like unique MGO.

Acknowledgements

We are grateful for the financial support by the Natural Science Foundation of China (51172039 and 51572044), the Fundamental Research Funds for the Central Universities of China (N130305001) and the Scientific Research Fund of Liaoning Provincial Education Department (L2014103 and LZ2015031).

References

1 Q. Li, J.O. Jensen, R.F. Savinell and N.J. Bjerrum, *Prog. Polym. Sci.*, 2009, **34**, 449-477.
2 H. Zhang and P.K. Shen,*Chem. Soc. Rev.*, 2012, **41**, 2382-.
3 J.A. Asensio, E.M. Sánchez and P. Gómez-Romero, *Chem. Soc. Rev.*, 2010, **39**, 3210-3239.
4 E. Quartarone and P. Mustarelli, *Energy Environ. Sci.*, 2012, **5**, 6436-6444.
5 S. Kang, C. Zhang, G. Xiao, D. Yan and G. Sun, *J. Membr. Sci.*, 2009, **334**, 91-100.
6 J. Jouanneau, R. Mercier, L. Gonon and G. Gebel, *Macromolecules*, 2007, **40**, 983-990.
7 J. Yang, D. Aili, Q. Li, Y. Xu, P. Liu, Q. Che, J.O. Jensen, N.J. Bjerrum and R. He, *Polym. Chem.*, 2013, **4**, 4768-4775.
8 J. Yang and R. He, *Polym. Adv. Technol.*, 2010, **21**, 874-880.
9 J. Yang, Q. Li, J.O. Jensen, C. Pan, L.N. Cleemann, N.J. Bjerrum and R. He, *J. Power Sources*, 2012, **205**, 114-121.
10 P. Mustarelli, E. Quartarone, S. Grandi, A. Carollo and A. Magistris, *Adv. Mater.*, 2008, **20**, 1339-1343.

11 Suryani, Y.-N. Chang, J.-Y. Lai and Y.-L. Liu, *J. Membr. Sci.*, 2012, **403-404**, 1-7.
12 D. Aili, T. Allward, S.M. Alfaro, C. Hartmann-Thompson, T. Steenberg, H.A. Hjuler, Q. Li, J.O. Jensen and E.J. Stark, *Electrochim. Acta*, 2014, **140**, 182-190.
13 S. Singha and T. Jana, *ACS Appl. Mater. Interfaces*, 2014, **6**, 21286-21296.
14 J. Lobato, P. Cañizares, M.A. Rodrigo, D. Úbeda and F.J. Pinar, *J. Membr. Sci.*, 2011, **369**, 105-111.
15 D. Plackett, A. Siu, Q. Li, C. Pan, J.O. Jensen, S.F. Nielsen, A.A. Permyakova and N.J. Bjerrum, **J. Membr. Sci.**, 2011, **383,** 78-87.
16 Suryani, C.M. Chang, Y.L. Liu, and Y.M. Lee, *J. Mater Chem.*, 2011, **21**, 7480-7486.
17 R. Kannan, H.N. Kagalwala, H.D. Chaudhari, U.K. Kharul, S. Kurungot, and V.K. Pillai, *J. Mater. Chem.*, 2011, **21**, 7223-7231.
18 C. Xu, Y. Cao, R. Kumar, X. Wu, X. Wang and K. Scott, *J. Mater. Chem.*, 2011, **21**, 11359-11364.
19 Y. Wang, Z. Shi, J. Fang, H.Xu, X. Ma, and J. Yin, *J. Mater. Chem.*, 2011, **21**, 505-512.
20 L. Dai, *Acc. Chem. Res.*, 2012, **46**, 31-42.
21 M.R. Karim, K. Hatakeyama, T. Matsui, H. Takehira, T. Taniguchi, M. Koinuma, Y. Matsumoto, T. Akutagawa, T. Nakamura, S. Noro, T. Yamada, H. Kitagawa and S. Hayami, *J. Am. Chem. Soc.*, 2013, **135**, 8097-8100.
22 H. Zarrin, D. Higgins, Y. Jun, Z. Chen and M. Fowler, *J. Phys. Chem. C*, 2011, **115**, 20774-20781.
23 C. Xu, X. Liu, J. Cheng and K. Scott, *J. Power Sources*, 2015, **274**, 922-927.
24 N. Zhang, B. Wang, Y. Zhang, F. Bu, Y. Cui, X. Li,C. Zhao and H. Na, *Chem. Commun.*, 2014, **50**, 15381-15384.
25 Y.-S. Ye, C.-Y. Tseng, W.-C.Shen, J.-S. Wang, K.-J. Chen, M.-Yao Cheng, J. Rick, Y.-J. Huang, F.-C. Chang and B.-J. Hwang, *J. Mater. Chem.*, 2011, **21**, 10448-10453.
26 Y. He, J. Wang, H. Zhang, T. Zhang, B. Zhang, S. Cao and J. Liu, *J. Mater. Chem. A*, 2014, **2**, 9548-9558.
27 W. S. Hummers and R.E. Offeman, *J. Am. Chem. Soc.*, 1958, **80**, 1339.
28 J. Liu, G. Chen and M. Jiang, *Macromolecules*, 2011, **44**, 7682-7691.
29 H. Yang, C. Shan, F. Li, D. Han, Q. Zhang and L. Niu, *Chem. Commun.*, 2009, **26**, 3880-3882.
30 J. Yang, L.N. Cleemann, T. Steenberg, C. Terkelsen, Q. Li, J.O. Jensen, H.A. Hjuler, N.J. Bjerrum and R.H. He, *Fuel Cells*, 2014, **14**, 7-15.
31 A. Lerf, H. He, M. Forster and J. Klinowski, *J. Phys. Chem. B*, 1998, **102**, 4477-4482.
32 G. Eda and M. Chhowalla, *Adv. Mater.*, 2010, **22**, 2392-2415.
33 C. Xue, J. Zou, Z. Sun, F. Wang, K. Han and H. Zhu, *Int. J. Hydrogen Energy*, 2014, **39**, 7931-7939.
34 D. Aili, L. N. Cleemann, Q. Li, J. O. Jensen, E. Christensen and N. J. Bjerrum, *J. Mater. Chem.*, 2012, **22**, 5444-5453.

Novel composite membranes of triazole modified graphene oxide and polybenzimidazole for high temperature polymer electrolyte membrane fuel cell applications

Jingshuai Yang, Chao Liu, Liping Gao, Jin Wang, Yixin Xu, Ronghuan He*

Novel acid-doped membranes possessing improved proton conductivity and enhanced mechanical properties were prepared from polybenzimidazole and triazole modified graphene oxide.